ELSEVIER

Journal of Biomechanics 36 (2003) 53–62

JOURNAL OF BIOMECHANICS

www.elsevier.com/locate/jbiomech
www.JBiomech.com

Stroke frequency in front crawl: its mechanical link to the fluid forces required in non-propulsive directions

Toshimasa Yanai*

School of Physical Education, University of Otago, P.O. Box 56, Dunedin, New Zealand

Accepted 14 August 2002

Abstract

Two hypotheses were tested: (a) stroke frequency is predictable from the amplitudes of bodyroll and the turning effect around the body's long-axis generated by the non-propulsive fluid forces (that is, the torque driving bodyroll), and (b) swimmers exhibit at least one alteration in the factors influencing the bodyroll cycle as they increase the stroke frequency for faster swimming, so that they can reduce the fluid forces "wasted" in non-propulsive directions. The mechanical formula that links stroke frequency and the kinetics of bodyroll was derived on the basis of Euler's equation of motion. Experimental data were collected from competitive swimmers to validate the derived mechanical relations and to examine the strategy that skilled swimmers would use to change the stroke frequency as they swam faster. A strong correlation (slow: $r = 0.70$ and fast: $r = 0.85$) and a non-significant difference between the observed stroke frequency and the formula-based estimates supported the first hypothesis. As the subjects increased stroke frequency (38%) for faster swimming, bodyroll decreased (19%) and the trunk twist increased (40%). The combined alterations resulted in a small reduction in the shoulder roll (12%), enabling the swimmers to gain the benefits associated with a large rolling action of the upper trunk, while limiting the amount of increase in the turning effect of fluid forces in non-propulsive directions (40%). The second hypothesis was, therefore, supported. The derived mechanical formula provides a theoretical basis to explore mechanisms underlying the interrelations among stroke frequency, stroke length and swimming speed, and sheds light on a possible reason that swimmers generally adopt six-beat kicks.

Keywords: Bodyroll; Euler's equation of motion; Principal moment of inertia; Six-beat kick; Three-dimensional videography

1. Introduction

Front crawl is the fastest form of human locomotion in an aquatic environment. The world records in the freestyle events, in which most swimmers, if not all, use the front crawl technique, demonstrate the level of sophistication in the skill of human locomotion in water. Competitive swimmers train to use the complex time- and position-dependent fluid force system effectively, so that they can maximize the distance travelled with one stroke cycle (stroke length) and the rate at which the stroke cycle is repeated (stroke frequency). The stroke length and stroke frequency of competitive swimmers have been investigated by many researchers (Arellano et al., 1994; Costill et al., 1991; Craig and Pendergast, 1979; Craig et al., 1985; East, 1970; Hay et al., 1983; Kennedy et al., 1990; Pai et al., 1984; Wakayoshi et al., 1993), the results of which suggest that a given swimmer swims faster in short term (e.g. on a given day) by increasing stroke frequency and that the same swimmer improves the maximum swimming speed in long term (e.g. over a season of training) by increasing the stroke length (Hay, 1993). The latter implies that the swimmers learn over a period to swim at a given speed with a reduced stroke frequency.

Intuitively, stroke frequency seems to be determined by the swimmer's internal effort of moving the arms at a desired frequency. Hay (1993) listed three factors as major determinants of stroke frequency: (a) the moment of inertia of the arm about the shoulder, (b) the range of motion through which the arm moves and (c) the torque applied to the arm through the shoulder. In front crawl, however, modifications of these three factors may not guarantee an increase in the stroke frequency because the arm movement in front crawl must be incorporated

*Fax: +64-3-479-8309.
E-mail address: tyanai@pooka.otago.ac.nz (T. Yanai).

0021-9290/02/$ - see front matter © 2002 Elsevier Science Ltd. All rights reserved.
PII: S0021-9290(02)00299-3

with the rolling action of the trunk about its long axis. An increase in stroke frequency must, therefore, be accompanied by a corresponding increase in the frequency of the trunk roll cycle.

The trunk roll is driven by two distinct sources of torque (Fig. 1): The turning effect of external (fluid) forces that generates the rolling of the entire body with respect to the global reference frame and the turning effect of internal forces that generates the rolling of the trunk relative to the principal axes of the entire body. Yanai (2001) found that the trunk roll exhibited by competitive swimmers was attributed primarily to the turning effect of the external forces rather than that of the internal forces. This result indicates that competitive swimmers generate, consciously or unconsciously, a suitable amount of external force to match the rolling cycle of the entire body with the arm movement cycle. Because the external forces that generate the roll of the entire body must act in vertical or medio-lateral directions (non-propulsive directions), the required matching imposes a constraint on the swimmers that may limit swimming propulsion and efficiency. This line of logic sheds additional light on the mechanism of interrelations among stroke frequency, stroke length and swimming speed, providing a foundation to advance the level of sophistication of front crawl technique. Two hypotheses were tested in the present study: (a) stroke frequency is predictable from the amplitudes of bodyroll and the turning effect around the body's long-axis generated by the non-propulsive fluid forces and (b) swimmers exhibit at least one alteration in the factors influencing the bodyroll cycle as they increase the stroke frequency for faster swimming, so that they can reduce the fluid forces "wasted" in non-propulsive directions.

2. Methods

In the present study, the term "bodyroll" described the rolling action of the swimmer's body due to the turning effect of the external (fluid) forces (Fig. 1, center). Specifically, the angular displacement of the entire body about its longest principal axis defined bodyroll. Although the definition of the swimmer's whole body angular displacement had only a conceptual, but no physical, significance because of a swimming human body not being a single rigid system, an effort was made to calculate a single representative value of "bodyroll" that could allow an establishment of mechanical link between the stroke frequency and the turning effect around the long-axis generated by the fluid forces, and comparisons across subjects (computational details are described later).

The mechanical link between the stroke frequency and the turning effect of fluid forces required for a given rolling cycle of the entire body was defined on the basis of Euler's equation of motion in four steps: First, the bodyroll cycle was modeled and expressed as an angular displacement vs. time relation. As apparent from the movement pattern of front crawl, bodyroll was expected to exhibit a sinusoidal pattern of change with respect to time (Fig. 2), expressed as

$$\mathrm{Bodyroll}(t) = \mathrm{BR}_{\mathrm{MAX}} \sin(2\pi t/T), \tag{1}$$

where $\mathrm{BR}_{\max}$ is the maximum bodyroll angle (rad), T the stroke time (s) and t the time measured with respect to an instant at which Bodyroll $= 0$.

Second, the moment of inertia of the entire body about the long-axis, $J_{\mathrm{L}}(t)$, was modeled. Its changing pattern should exhibit two cycles in a stroke as the body

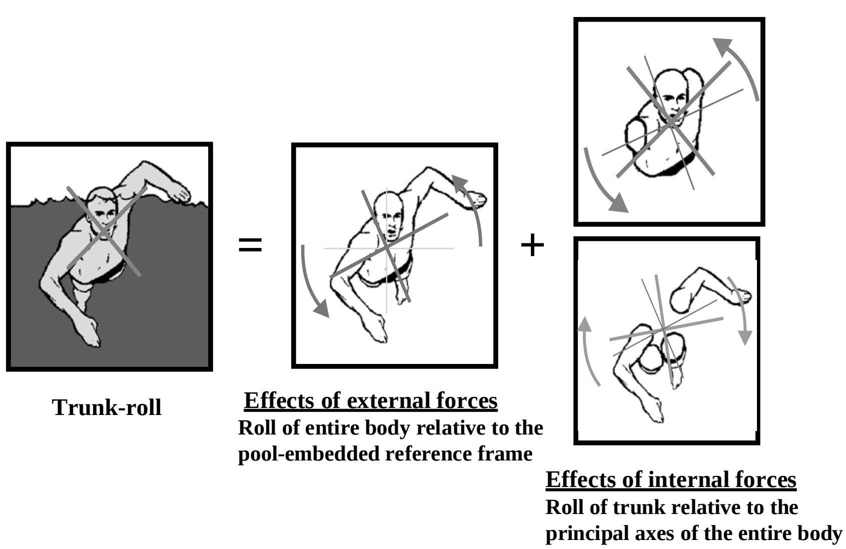

Fig. 1. Two sources of torque that drive trunk roll. First, the turning effect of external (fluid) forces acting on the body that causes the entire body to roll with respect to the global frame of reference; and second, the turning effect of internal forces acting within the body that causes the trunk to roll with respect to the principal axes of the entire body. In the present study, the rolling action of the entire body due to the fluid forces is defined as bodyroll.

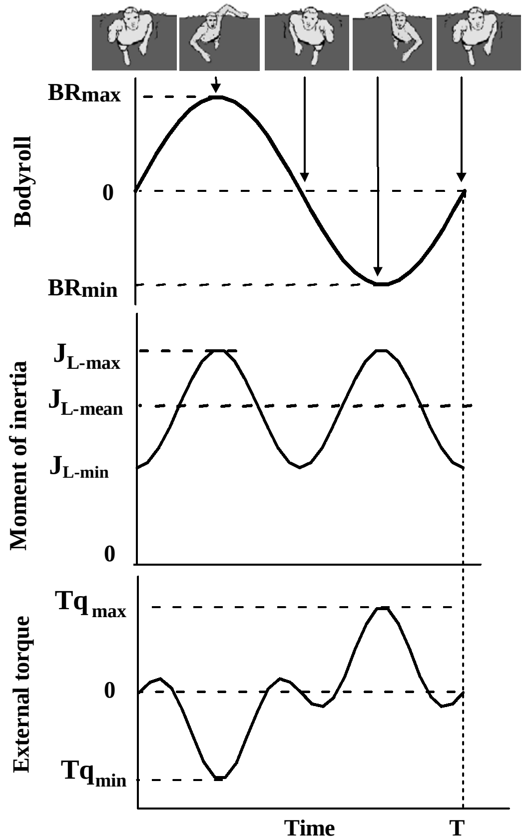

Fig. 2. The modeled changing pattern of bodyroll, whole body moment of inertia about the long-axis, and the turning effect of the external forces (external torque) for a complete stroke cycle. As apparent from the illustrations of a swimmer in the view from the front, bodyroll was expected to exhibit a sinusoidal pattern of change at the stroke frequency. The changing pattern of whole body moment of inertia was expected to exhibit two sinusoidal patterns in a stroke cycle as the body mass distributes away from the long axis during the two recovery phases. The external torque was derived analytically as the first time derivative of the product of the angular velocity of bodyroll and the moment of inertia.

mass distributes away from the long-axis during the two recovery phases (Fig. 2). Thus,

$$J_L(t) = J_{L\text{-MEAN}} - J_{L\text{-AMP}} \cos(4\pi t/T + \beta), \tag{2}$$

where $J_{L\text{-MEAN}}$ is the mean value, $J_{L\text{-AMP}}$ the amplitude of the fluctuating moment of inertia [$J_{L\text{-}AMP} = \frac{1}{2}(J_{L\text{-MAX}} - J_{L\text{-MIN}})$] and β the phase lag between $J_L(t)$ and Bodyroll(t).

Third, the turning effect of fluid forces [Tq(t)] was analytically derived as follows:

$$\mathrm{Tq}(t) = \mathrm{d}(J_L\omega_L)/\mathrm{d}t - (J_F - J_T)\omega_T\omega_F, \tag{3}$$

where ω_L, ω_F and ω_T are the angular velocities of the entire body about long, frontal and transverse axes, respectively, and J_F and J_T are the moments of inertia about frontal and transverse axes, respectively. Because the product of the angular velocities ω_T and ω_F was expected to be small in front crawl, the second term on the right-hand side of the equation was assumed to be zero. This assumption made the effect of fluctuating J_F and J_T of the swimmers on the torque insignificant. Replacing ω_L by ω_{BR} the angular velocity of bodyroll [= d Bodyroll(t)/dt] resulted in:

$$\begin{aligned}\mathrm{Tq}(t) = &- J_{L\text{-MEAN}}\mathrm{BR_{MAX}}(2\pi/T)^2 \sin(2\pi t/T)\\ &+ 5J_{L\text{-AMP}}\mathrm{BR_{MAX}}(2\pi/T)^2 \sin(2\pi t/T)\cos\beta\\ &- 6J_{L\text{-AMP}}\mathrm{BR_{MAX}}(2\pi/T)^2 \sin^3(2\pi t/T)\cos\beta\\ &+ 2J_{L\text{-AMP}}\mathrm{BR_{MAX}}(2\pi/T)^2 \cos(2\pi t/T)\sin\beta\\ &- 6J_{L\text{-AMP}}\mathrm{BR_{MAX}}(2\pi/T)^2 \sin^2(2\pi t/T)\\ &\cos(2\pi t/T)\sin\beta.\end{aligned} \tag{4}$$

Finally, the formula at the global maximum ($t = T/4$) with zero phase lag ($\beta = 0$) was extracted and rearranged into a simple formula that expressed the mechanical link between the stroke frequency and the turning effect of fluid forces around the body's long-axis,

$$\mathrm{SF} = \frac{1}{T} = \frac{1}{2\pi}\sqrt{\frac{\mathrm{Tq_{MAX}}}{[\mathrm{J_{L\text{-MEAN}}} + J_{L\text{-AMP}}]\mathrm{BR_{MAX}}}}. \tag{5}$$

This formula dictates that stroke frequency (SF) is proportional to the square root of the turning effect of fluid forces ($\mathrm{Tq_{MAX}}$) and inversely proportional to the square root of the maximum bodyroll ($\mathrm{BR_{MAX}}$).

An experiment was conducted to test the validity of the derived mechanical formula and to examine the strategy that swimmers used to change the stroke frequency. A three-dimensional videography technique with panning periscopes (Yanai et al., 1996) was used for the data collection. Eleven members of a collegiate men's swimming team were asked to perform front-crawl at a moderate pace (speed = 1.3 ± 0.1 m/s) and a sub-maximum sprinting pace (speed = 1.6 ± 0.1 m/s). No instruction was given to the subjects regarding the stroke frequency, so that they were able to adopt the stroke frequency that they felt comfortable and natural for the given speeds of performance. The performances were recorded by camcorders (Panasonic AG 450-SVHS) fixed to the respective periscopes (Fig. 3). The periscopes were located approximately 20 m away from the subjects, and the distortion of the recorded images due to refraction (Kwon, 1999) was minimal. The procedure for data collection was approved by the Human Subject Review Committee and each subject provided written informed consent.

The videotapes of the performances were manually digitized for every field (60 fields/s) using a Peak 2D System (Peak Performance Technologies, Denver, CO, USA) for one stroke cycle. In each field, 21 body landmarks were digitized to represent the end points of each of 14 segments of a human body model which consisted of head, torso, upper arms, forearms, hands, thighs, shanks and feet (digitize–redigitize reliability was

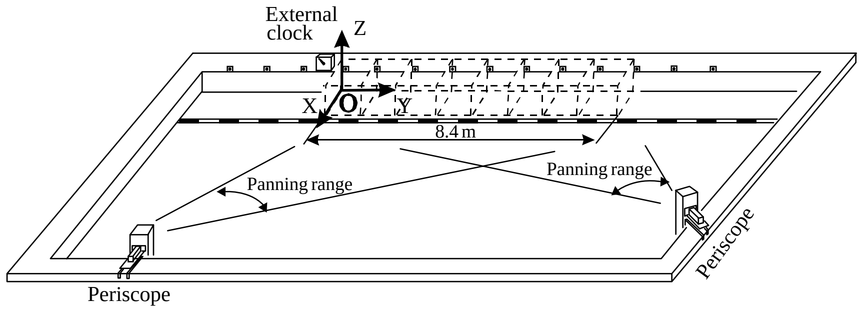

Fig. 3. Diagram of experimental set-up for data collection. The volume indicated by dashed lines is the total object space of $1.5 \times 8.4 \times 2.0$ m^3. Each subsection of the total object space indicates a single space calibrated by locating the control object. Fourteen wooden blocks were placed on the pooldeck and served as reference markers. The included angles of imaginary lines connecting each body landmark to the two periscopes, projected on the horizontal plane, ranged from 54° to 67°. The external clock, whose angular speed was roughly 20 revolution/s, was started and stopped immediately before and after each trial, while both cameras were recording the clock. The recorded image of the clock-arm was used to match fields for the two cameras for video synchronization.

high [$r > 0.98$]). The resulting sets of two-dimensional coordinate data were then transformed into the corresponding three-dimensional coordinates on the basis of a DLT-based algorithm (Yanai et al., 1996). The length of each segment determined from the video recordings was subject to a mean error of $<3\%$. The coordinates were expressed with respect to a global reference frame (GRF) with origin 'O' located at the surface level of the pool when the water was still and undisturbed (Fig. 3). The three-dimensional coordinates were smoothed using a fourth order, zero lag, low-pass Butterworth filter (Winter et al., 1974) with various cut-off frequencies (2–4 Hz). The cut-off frequencies were set so that approximately 95% ($\pm 3\%$) of the power of the original signal could be retained in the filtered signal.

The 3×3 mass–center inertia matrix of the entire body about three orthogonal axes parallel to the GRF and passing through the CM (J_{CM}) was determined from the following equation (Haug, 1992):

$$J_{\mathrm{CM}} = \sum_{i=1}^{14} (A_{i/\mathrm{GRF}} J_i A_{i/\mathrm{GRF}}^{\mathrm{T}} + m_i (r_{i/\mathrm{CM}}^{\mathrm{T}} r_{i/\mathrm{CM}} I - r_{i/\mathrm{CM}} r_{i/\mathrm{CM}}^{\mathrm{T}})), \tag{6}$$

where $A_{i/\mathrm{GRF}}$ is the 3×3 rotation matrix to represent the orientation of the segment i with respect to the GRF, J_i the 3×3 diagonal matrix for the principal moment of inertia of segment i, m_i the mass of the segment i, $r_{i/\mathrm{CM}}$ the position vector pointing from the whole body center of mass to the center of mass of the segment i, and I the 3×3 identity matrix.

All body segments were assumed to be symmetric about their own long axes. The principal moment of inertia of each body segment (J_i) required for the computation was estimated by normalizing and scaling the data presented by Whitsett (1963) in accordance with the method described by Dapena (1978). The segmental masses and the relative position of each segmental CM were estimated from the data presented by Clauser et al. (1969) and Hinrichs (1990). The moment of inertia of the entire body about its long axis (J_{L}) and the unit vector representing the long axis of the entire body were determined for every field as the smallest eigenvalue of J_{CM} and the corresponding eigenvector, respectively. A computer subroutine "jacobi" (Press et al., 1992, pp. 460–461) was used for this computation.

Bodyroll was determined for every field as the time integral of the angular velocity of the entire body about the long axis, which, in turn, was determined from the angular momentum of the entire body about the long axis and the J_{L}. The determined bodyroll, therefore, represented the angular displacement that a single rigid body possessing the same mass and mass distribution as the swimmer's body would have to exhibit in order to have the same angular momentum about the CM of the body that the swimmer's body possessed. The initial value for the integration was chosen, so that the mean value of bodyroll over one complete cycle became zero. The turning effect of the fluid forces around the long axis was determined as the dot product of the time derivative of the angular momentum vector and the unit vector representing the long axis. The angular momentum of the entire body about three orthogonal axes passing through the CM was computed with the procedure described by Dapena (1978) with two modifications. First, the trunk segment was subdivided mathematically into two sections—upper and lower halves—connected through the mutual long-axis. Each of the two sections had an identical value for the moment of inertia about the center of mass of the entire trunk ($J_{\mathrm{Trunk}}/2$). The rotations of the upper and lower halves of the trunk about the long-axis were determined as shoulder roll (SR) and hip roll (HR) angles, respectively. The angular momentum of the entire trunk about its long axis (H_{Trunk}) was therefore determined as follows:

$$H_{\mathrm{Trunk}} = [J_{\mathrm{Trunk}}(\omega_{\mathrm{SR}} + \omega_{\mathrm{HR}})/2], \tag{7}$$

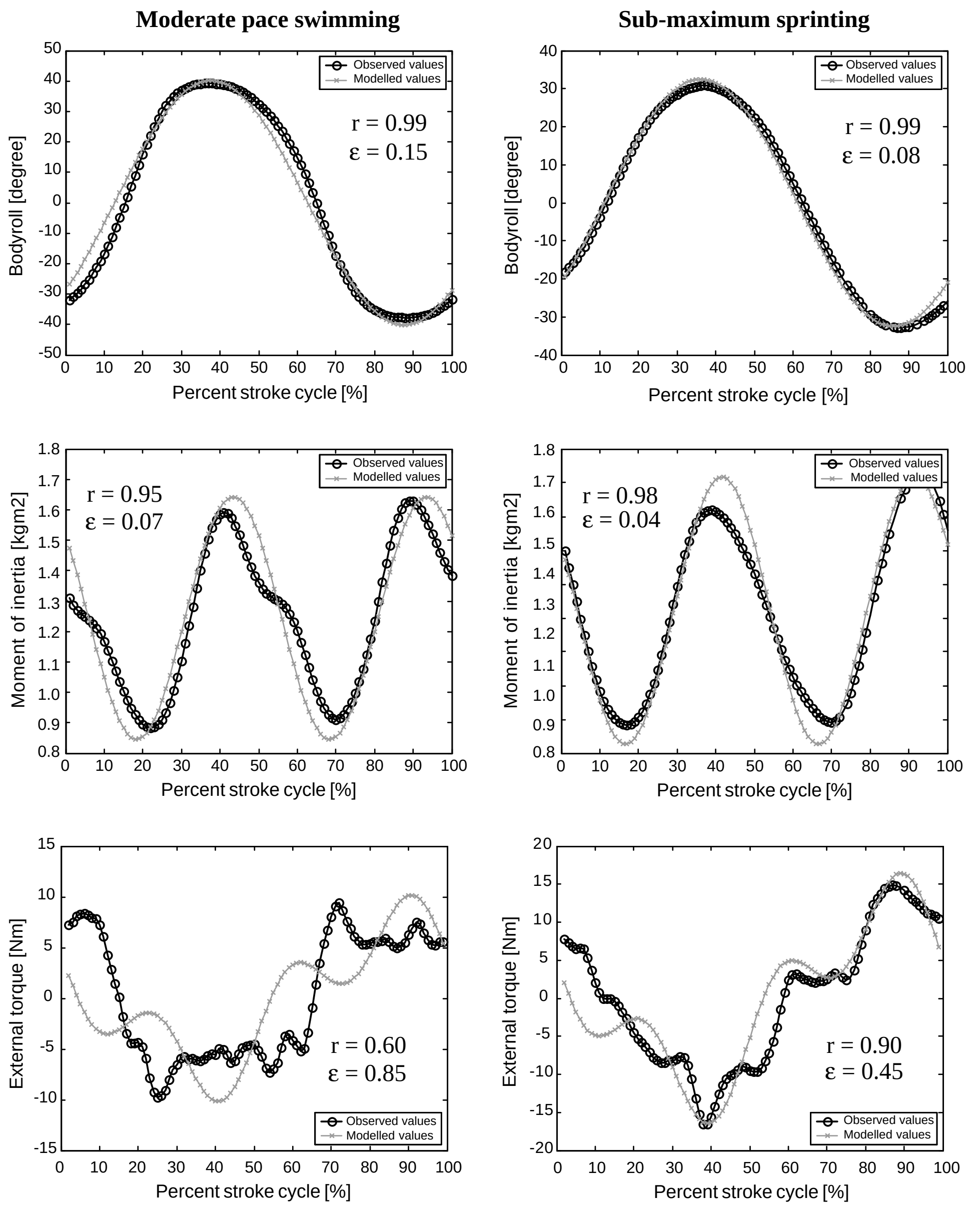

Fig. 4. The changing pattern across subjects for bodyroll (top), whole body moment of inertia (middle) and external torque (bottom) for moderate pace swimming (left) and sub-maximal sprinting (right) for one stroke cycle. Each set of time-series data represents the average values across all subjects for time-normalized, phase-adjusted data: time was normalized with respect to the stroke time for each subject, and the phase was adjusted using cross-correlation analysis to have the bodyroll cycle synchronized for all subjects (the phase difference between bodyroll cycle and moment of inertia cycle was not adjusted). (Note: The maximum and minimum values attained in the observed data were not identical to the corresponding values in the modeled data because: (a) the average value over the stroke cycle for a given observed data set was not necessarily equal to the average between the maximum and minimum values taken from the same data set, and (b) the instants at which a series of maximum and minimum values were attained in the observed data were not always identical to the corresponding instants in the modeled data, and the difference in timing of these instants was not constant across subjects even after the phase adjustment.) The time-series data modeled with the mechanical formulae matched closely the corresponding data obtained experimentally, indicating that the changing patterns of the variables were well represented by the simple mechanical functions. The *r*-values are correlation coefficients between the observed and modeled data and the ε-values indicate the relative difference between the two for the ith field computed with the following formula:

$$\sqrt{\frac{\sum(\text{Modelled}_i - \text{Observed}_i)^2}{\sum \text{Observed}_i^2}}.$$

where ω_{SR} and ω_{HR} are the angular velocities of SR and HR, respectively.

The second modification was that the angular velocities of the head and limb segments about their long axes were not assumed to be zero but estimated from the angular velocity of the trunk, in accordance with the method described by Dapena (1997).

The validity of the mechanical formula that links the stroke frequency and the turning effect of fluid forces (Eq. (5)) was tested by comparing the experimentally obtained values of stroke frequency with the formula-based estimates by means of correlation analysis and paired t-test. The standard formula [$\mathrm{SF} = 1/T$] was used to determine the experimental value of stroke frequency. The stroke time (T) in this computation was measured as the duration between two successive arm entries on the same side. The formula-based estimates were determined with four experimentally determined bodyroll-related variables ($\mathrm{BR_{MAX}}$, $J_{\text{L-MEAN}}$, $J_{\text{L-AMP}}$ and $\mathrm{Tq_{MAX}}$) as input. The strategy that the swimmers used to change the stroke frequency was determined by conducting a series of paired t-tests for seven bodyroll-related variables (those listed above plus $\mathrm{Tq_{MAX}}$, $\mathrm{SR_{MAX}}$, $\mathrm{HR_{MAX}}$) obtained for two swimming speeds. The statistical significance was assessed at 0.05 level.

3. Results

The mechanical formula was found valid and the stroke frequency was predicted well with a mechanical formula that involves the turning effect around the body's long axis generated by the fluid forces in non-propulsive directions. All three time-series variables modeled with the mechanical formulae were highly correlated with the corresponding variables obtained for sub-maximal sprinting trials ($r > 0.90$), whereas the correlation was slightly weaker ($r > 0.60$) for moderate pace trials (Fig. 4). A strong correlation (Fig. 5) was found between the observed and the estimated stroke frequencies for both moderate pace ($r = 0.70$) and sub-maximal sprint pace ($r = 0.85$), and the mean difference between the observed and estimated stroke frequencies (Table 1) were not significantly different from zero. These results support the first hypothesis.

As the subjects increased their stroke frequency (by 38%) for the faster swimming pace, bodyroll was decreased by 19% (Table 2) and the trunk twist increased by 40% (Table 3). This combination of changes resulted in a small reduction in the shoulder roll (by 12%) and a limited increase in the magnitude of external torque (by 40%). The mechanical formula (Eq. (5)) indicate that the observed reduction in bodyroll has contributed to reducing the external torque required as the increased stroke frequency, and thereby, the second hypothesis is supported.

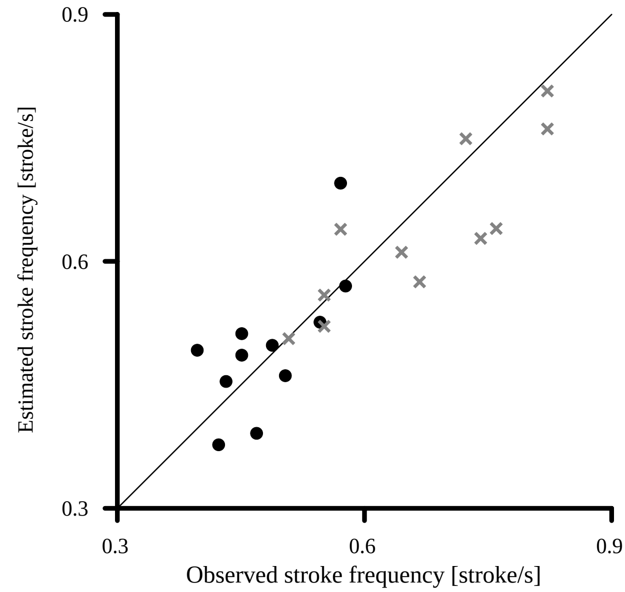

Fig. 5. Correlation between the observed and estimated stroke frequencies. Each plot indicates a data set for each subject for moderate pace swimming (•) and sub-maximal sprinting (×). Strong correlations ($r = 0.70$ for moderate pace and $r = 0.85$ for sub-maximum sprinting) indicate that the variance in the stroke frequency can be explained primarily by the variances in the amplitude of bodyroll, the whole body moment of inertia and the turning effect of external forces acting on the swimmer. The slope of the regression equation passing through the origin (1.04 for distance pace and 0.95 for sub-maximum sprinting) was not significantly different from 1.0, indicating that the stroke frequency was predictable with a mechanical formula describing the kinetics of bodyroll cycle.

4. Discussion

Observations have consistently suggested that swimmers improve their performance over a period of training, being able to attain a faster speed with an increased stroke length: In other words, swimmers learn to swim at a given speed with a reduced stroke frequency. The present study was conducted to establish a mechanical foundation that linked the stroke frequency of front-crawl and the fluid forces required in non-propulsive directions, so that underlying mechanism of the observed interrelations among stroke frequency, stroke length and speed could be examined.

The methods used in the study involved three limitations: First, the mechanical formulae were derived on the basis of two-dimensional angular motion of the body with an assumption that the movements of the entire body about its frontal and transverse axes were small and the effect of it on the kinetics of bodyroll was negligible. This assumption was supported by the experimental data demonstrating that the entire body changed its orientation only by ± 0.02 rad at < 0.32 rad/s about the frontal-axis (ω_F) and ± 0.07 rad at < 0.15 rad/s about the transverse axis (ω_T), with a negligible effect on the kinetics of bodyroll. Hence, the application of two-dimensional analysis for bodyroll was justified. Second, the phase lag between the bodyroll cycle and the cycle of moment of inertia was assumed to be zero for the derivation of the formula that predicted

Table 1
Observed and estimated stroke frequencies (strokes/s)

	Moderate pace			Sub-maximum sprinting		
	Observed	Estimated	Difference	Observed	Estimated	Difference
1	0.571	0.695	−0.123	0.723	0.749	−0.026
2	0.469	0.391	0.078	0.741	0.628	0.113
3	0.451	0.486	−0.034	0.645	0.611	0.034
4	0.504	0.461	0.043	0.822	0.761	0.061
5	0.397	0.492	−0.095	0.508	0.506	0.002
6	0.488	0.498	−0.010	0.667	0.575	0.091
7	0.451	0.512	−0.061	0.571	0.639	−0.068
8	0.423	0.377	0.045	0.551	0.559	−0.009
9	0.432	0.454	−0.022	0.551	0.521	0.030
10	0.577	0.570	0.007	0.760	0.640	0.119
11	0.546	0.526	0.019	0.822	0.807	0.015
Mean	0.4826	0.4964	−0.014	0.6691	0.6360	0.033
	(0.442 0.523)	(0.438 −0.554)	(−0.055–0.028)	(0.593 −0.745)	(0.570 −0.702)	(−0.006–0.073)

Note. The values in parentheses indicate the 95% confidence intervals.

Table 2
The factors influencing bodyroll and factors influencing arm movements for two swimming paces

	Moderate pace	Sub-maximum sprinting	% Change
Speed (m/s)	1.30	1.59	+22*
	(1.23–1.36)	(1.49–1.68)	
Stroke frequency (stroke/s)	0.48	0.67	+39*
	(0.44–0.52)	(0.59–0.75)	
BR_{MAX} (rad)	0.70	0.57	−21*
	(0.61–0.79)	(0.49–0.64)	
$J_{L\text{-}MEAN}$ (kg m^2)	1.24	1.32	+6*
	(1.08–1.41)	(1.16–1.48)	
$J_{L\text{-}AMP}$ (kg m^2)	0.41	0.42	+2
	(0.35–0.47)	(0.36–0.49)	
Tq_{MAX} (N m)	15.9	22.4	+40*
	(12.7–19.1)	(19.1–25.7)	

Notes. The values in parentheses indicate the 95% confidence intervals.
*Indicates that the change in value was significantly different from zero at 0.05 level.

Table 3
Attributes of shoulder roll

	Moderate pace	Sub-maximum sprinting
Trunk twist	15° (20%)	21° (32%)
Roll of hip relative to body	19° (25%)	12° (18%)
Roll of entire body	41° (55%)	33° (50%)
Total (shoulder roll)	75° (100%)	66° (100%)

Note. The values in parentheses indicate the percent contribution to shoulder roll.

stroke frequency (Eq. (5)). On average, the phase lag was $3.6 \pm 1.9\%$ and $3.5 \pm 1.9\%$ of the stroke time for slow and fast trials, respectively. A sensitivity analysis (Fig. 6) indicated that the error in estimating stroke frequency due to the zero phase lag assumption was less than 0.002 strokes/s ($<0.3\%$) for a range of $\pm 10\%$ in phase lag. In addition, the experimental data demonstrated that the formula estimated the stroke frequency with a high accuracy even for the subject whose phase difference was largest (7% of stroke time). These data suggest that the derived formula presents a simple but valid mechanical relation between the stroke frequency and the kinetics of bodyroll. Third, the calculated bodyroll represented the angular displacement of the body's principal axes generated exclusively by the fluid forces acting on the entire body, and thus, possible angular displacement of the principal axes generated by other mechanism (Fig. 7) was not taken into account. This might explain why the observed amplitude of bodyroll was smaller than the amplitudes of shoulder and hip rolls (Table 3). However, it allowed derivation of a simple mechanical formula linking stroke frequency and the fluid forces required for bodyroll.

The present study demonstrated that a simple formula described well the mechanical relations between stroke frequency and the factors influencing bodyroll, and that the stroke frequency was predictable with the formula. This finding indicates that the stroke frequency is controlled not only by the swimmer's internal effort of moving the arms at a desired rate, but also by the swimmer's ability to generate the fluid forces in non-propulsive directions to match the frequency of the bodyroll cycle with that of the arm movement cycle. The formula dictates that an increase in the stroke frequency requires a corresponding increase in the turning effect of non-propulsive fluid forces unless the amplitude of bodyroll is reduced substantially (Eq. (5)). It suggests that swimmers should adopt the lowest stroke frequency possible at given speeds of swimming, because a lowered

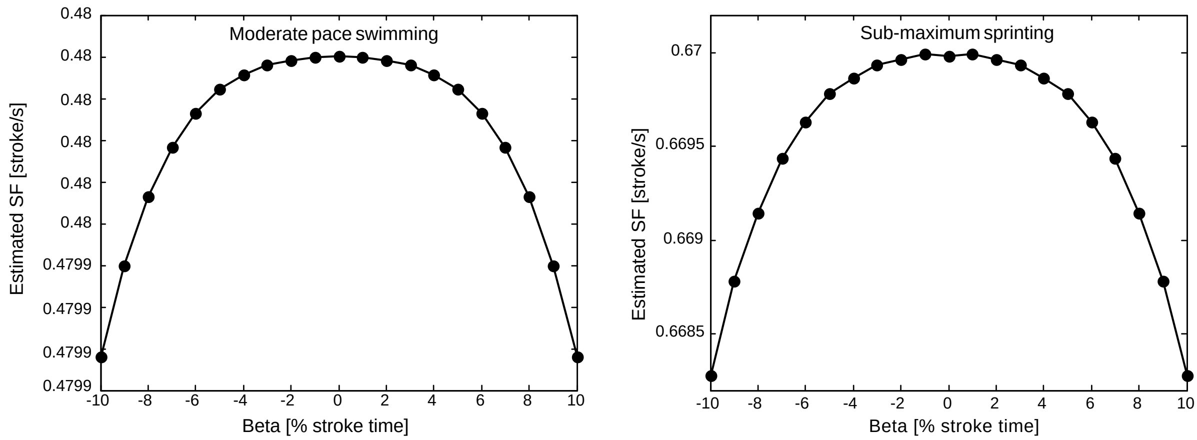

Fig. 6. The influence of the phase lag between the bodyroll and moment of inertia cycles on the estimation of stroke frequency. The influence was determined in two steps: (a) using Eq. (4)), Tq_{MAX} for given stroke frequency, $J_{L\text{-MEAN}}$, $J_{L\text{-AMP}}$ and BR_{MAX} (Table 2) was computed for various magnitudes of phase lag (from −10% to 10% of stroke time), and (b) the Tq_{MAX} computed with every given phase lag was used as input for Eq. (5) to determine the formula-based estimate of the stroke frequency. Because Eq. (5) was derived with zero-phase-lag assumption, the estimated stroke frequency should not match the stroke frequency used as input in (a) for the phase lag$\neq 0$. In other words, the difference between the input stroke frequency (0.48 and 0.67 stroke/s for moderate pace and sub-maximum sprinting, respectively) and the estimated stroke frequency depicted the error in the estimation of stroke frequency due to the zero phase lag assumption. The results showed that the range of phase lag observed in the present study (<7% stroke time) did not substantially affect the accuracy in the estimation of stroke frequency (error <0.2%).

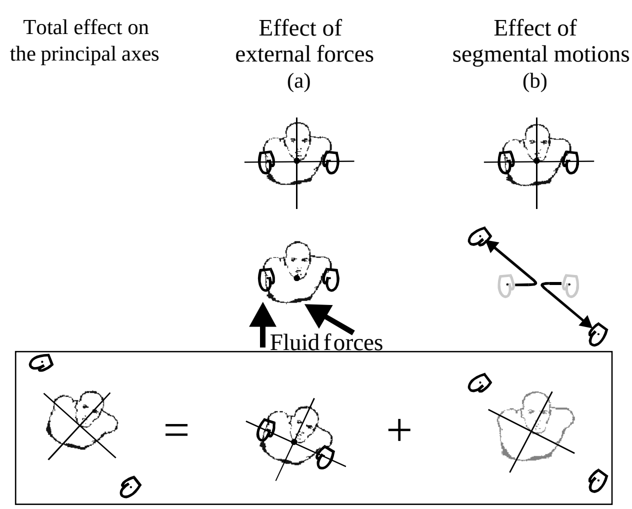

Fig. 7. Two mechanisms that generate angular displacement of the whole body principal axes around the long axis. The total angular displacement (left) consists of: (a) the component attributable to the turning effect of the fluid forces acting on the body (defined as bodyroll in the present study) and (b) the component attributable to linear motion of body segment(s) toward or away from the long axis (right). The mechanism of generating the latter component (b) is illustrated in the three figures in the right column. The initial body position is horizontally symmetric, having the body flat in a horizontal plane with the hands placed in symmetry (top). The hands start moving horizontally toward the long axis, maintaining the horizontal symmetry, and then, move away from the long-axis in oblique directions, disrupting the horizontal symmetry (middle). The final position of the hands is asymmetric, causing the principal axes to lean towards the left side of the body (bottom). This mechanism does not cause the rest of the body to roll in either direction because no rotational "action–reaction relationship" arises about the long axis as a result of the hand movements.

stroke frequency requires a reduced amount of fluid forces in the non-propulsive directions to maintain the same amplitude of bodyroll. This allows the swimmers to either increase the amplitude of bodyroll or learn to re-direct this surplus into the propulsive direction to swim faster. This postulated mechanism explains one possible reason for the observation that freestyle swimmers have improved their maximum swimming speed over a period of training by increasing their stroke lengths (Costill et al., 1991; Hay et al., 1983; Wakayoshi et al., 1993), because the observation indicates that the swimmers learned to swim at a given speed with a reduced stroke frequency. Longitudinal studies are indicated to examine the season-long changes in the stroke length–frequency relations and the propulsive efficiency, so that the above postulation can be evaluated.

The derived mechanical formula (Eq. (4)) provides a possible reason that swimmers generally adopt the so-called six-beat kick technique. With the six-beat kick technique, a downward thrust of the left leg coincides with the beginning of the recovery phase of the ipsilateral arm, the following downward thrust of the right leg is executed at the middle of the same recovery phase, and the second downward thrust of the left leg is executed at the entry of the ipsilateral arm into the water (Fig. 8). This pattern is repeated on the other side of the body during the recovery phase. The turning effect of the fluid forces generated by these kicks is expected to exhibit three sinusoidal cycles in a stroke cycle. One component of the derived mechanical formula that is a function of the fluctuating moment of inertia of the body has three sinusoidal cycles in a stroke cycle (Fig. 8). The timing of the three cycles and the six alternate directions of torque exactly match those expected from the six-beat kick technique. This perfect matching seems to explain why swimmers generally adopt six-beat kicks in front-crawl.

The present study also demonstrated that swimmers reduced the amplitude of bodyroll and increased the magnitude of trunk twist as they increased the stroke frequency for faster swimming. The increased trunk twist enabled the swimmers to attain a large rolling amplitude of the upper trunk (shoulder roll) so as to improve performance (Prichard, 1993) and to prevent shoulder injuries (Beekman and Hay, 1988; Ciullo and Stevens, 1989; McMaster, 1986; Neer and Welsh, 1977; Penny and Smith, 1980; Richardson et al., 1980). An increased trunk twist at high stroke frequency was also reported in a cross-sectional study of Olympic competitors (Cappaert et al., 1995), in which "sub-elite" swimmers exhibited a larger trunk twist (mean = 44°) at a higher stroke frequency (mean = 0.91 Hz) than "elite" swimmers (mean of 17° at 0.82 Hz), while both groups of swimmers attained nearly the same shoulder roll (mean of 35°). These findings suggest that competitive swimmers use the trunk-twisting motion effectively to gain the benefits associated with a large rolling action of the upper trunk and to prevent the amount of fluid forces "wasted" in non-propulsive directions for bodyroll from increasing as a quadratic function of stroke frequency (Eq. (5)). It is not certain, however, how much reduction in the fluid forces required for bodyroll optimizes the performance because: (a) some fluid forces may well be generated as a result of kicks and the buoyant force acting eccentric to the long-axis during the recovery phases and (b) a large trunk twist may increase the resistance acting on the swimmer. Further studies are indicated to examine the strategy for optimizing performance by reducing the fluid forces wasted in non-propulsive directions.

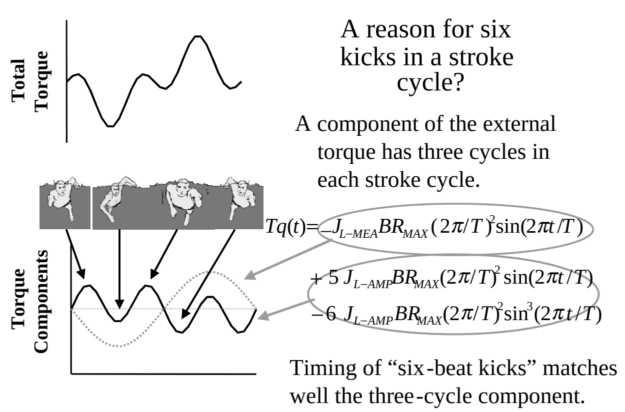

Fig. 8. A possible reason that swimmers generally, and somewhat naturally, adopt six-beat kicking technique in front crawl swimming. (Note: The Eq. (4) with zero phase lag ($\beta = 0$) is used in this figure for simplification purposes.) One component of the turning effect of external forces is a function of the body's fluctuating moment of inertia, which has three cycles in a stroke cycle. The timing of the three cycles and the six alternate directions of the torque exactly match those expected from the six-beat kick technique. For example, as the swimmer simultaneously kicks the left leg down and kicks the right up (first illustration), the hydrodynamic forces are expected to act upwards on the left leg and downwards on the right. These hydrodynamic forces generate a torque about the long-axis in the counter-clockwise (positive) direction in the view from the front. The bottom graph shows that this expected direction of the torque due to the kick matches the direction of torque indicated by the equation. This matching is also evident in the other five kicks executed in the same stroke cycle. It is postulated, therefore, that swimmers generally and naturally adopt six-beat kicks in front crawl, so that this component of torque can be generated by using the near-vertical fluid forces generated by kicks effectively, rather than by "wasting" the fluid forces generated by the arm strokes in non-propulsive directions.

The present study has established a mechanical foundation that links the stroke frequency in front crawl swimming and the fluid forces required in non-propulsive directions. This provides a theoretical basis to explore mechanisms underlying the interrelations among stroke frequency, stroke length and swimming speed that have been observed consistently over the years. Future studies are indicated to examine: (a) the influence of the non-propulsive fluid forces required to maintain the bodyroll cycle and propulsive efficiency and (b) the possible strategy to improve the technique of front crawl swimming by reducing the fluid forces wasted in non-propulsive directions.

References

Arellano, R., Brown, P., Cappaert, J., Nelson, R.C., 1994. Analysis of 50-, 100-, and 200-m freestyle swimmers at the 1992 Olympic games. Journal of Applied Biomechanics 10, 189–199.

Beekman, K.M., Hay, J.G., 1988. Characteristics of the front crawl techniques of swimmers with shoulder impingement syndrome. Journal of Swimming Research 4, 11–14.

Cappaert, J.M., Pease, D.L., Troup, J.P., 1995. Three-dimensional analysis of the men's 100-m freestyle during the 1992 Olympic games. Journal of Applied Biomechanics 11, 103–112.

Ciullo, J.V., Stevens, G.G., 1989. The prevention and treatment of injuries to the shoulder in swimming. Sports Medicine 7, 182–204.

Clauser, C.E., McConville, J.T., Young, J.W., 1969. Weight, Volume, and Center of Mass of Segments of the Human Body. Wright–Patterson Air Force Base, OH.

Costill, D.L., Thomas, R., Robergs, A., Pascoe, D., Lambert, C., Barr, S., Fink, W.J., 1991. Adaptations to swimming training: influence of training volume. Medicine and Science in Sports and Exercise 23, 371–377.

Craig, A.B., Pendergast, D.R., 1979. Relationship of stroke rate, distance per stroke, and velocity in competitive swimming. Medicine and Science in Sports and Exercise 11, 278–283.

Craig, A.G., Skehan, P.L., Pawelczyk, J.A., Boomer, W.L., 1985. Velocity, stroke rate, and distance per stroke during elite swimming competition. Medicine and Science in Sports and Exercise 17, 625–634.

Dapena, J., 1978. A method to determine the angular momentum of a human body about three orthogonal axes passing through its center of gravity. Journal of Biomechanics 11, 251–256.

Dapena, J., 1997. Contributions of angular momentum and catting to the twist rotation in high jumping. Journal of Applied Biomechanics 13, 239–253.

East, D.J., 1970. Swimming: an analysis of stroke frequency, stroke length and performance. New Zealand Journal of Health, Physical Education and Recreation 3, 16–25.

Haug, E.J., 1992. Intermediate Dynamics. Englewood Cliffs, NJ: Prentice-Hall.

Hay, J.G., 1993. The Biomechanics of Sports Techniques, 4th Edition. Englewood Cliffs, NJ: Prentice-Hall.

Hay, J.G., Guimaraes, A.C.S., Grimston, S.K., 1983. A quantitative look at swimming biomechanics. Swimming Technique 20, 11–17.

Hinrichs, R.N., 1990. Adjustments to the segment center of mass proportions of Clauser et al. (1969). Journal of Biomechanics 23, 949–951.

Kennedy, P., Brown, P., Chengalur, S.N., Nelson, R.C., 1990. Analysis of male and female Olympic swimmers in the 100-m events. International Journal of Sport Biomechanics 6, 187–197.

Kwon, Y.-H., 1999. Object plane deformation due to refraction in two-dimensional underwater motion analysis. Journal of Applied Biomechanics 15, 396–403.

McMaster, W.C., 1986. Painful shoulder in swimmers: a diagnostic challenge. Physician and Sportsmedicine 14, 108–122.

Neer, C.S., Welsh, R.P., 1977. The shoulder in sports. Orthopaedic Clinics in North America 8, 583–591.

Pai, Y.-C., Hay, J.G., Wilson, B.D., 1984. Stroking techniques of elite swimmers. Journal of Sports Science 2, 225–239.

Penny, J.N., Smith, C., 1980. Prevention and treatment of swimmer's shoulder. Canadian Journal of Applied Sport Science 5, 195–202.

Press, W.H., Teukolsky, S.A., Vetterling, W.T., Flannery, B.P., 1992. Numerical Recipes in Fortran: the Art of Scientific Computing, 2nd Edition. Cambridge University Press, Cambridge, UK.

Prichard, B., 1993. A new swim paradigm: swimmers generate propulsion from the hip. Swimming Technique 30, 17–23.

Richardson, A.B., Jobe, R.W., Collins, H.R., 1980. The shoulder in competitive swimming. American Journal of Sports Medicine 18, 159–163.

Wakayoshi, K., Yoshida, T., Ikuta, Y., Mutoh, Y., Miyashita, M., 1993. Adaptations to 6 months of aerobic swim training: changes in velocity, stroke rate, stroke length and blood lactate. International Journal of Sports Medicine 14, 368–372.

Whitsett, C.E., 1963. Some Dynamic Response Characteristics of Weightless Man (AMRL Technical Report 63-18). Wright–Patterson Air Force Base, OH.

Winter, D.A., Didwall, H.G., Hobson, D.A., 1974. Measurement and reduction of noise in kinematics of locomotion. Journal of Biomechanics 7, 157–159.

Yanai, T., 2001. What causes body to roll in front crawl swimming? Journal of Applied Biomechanics 17, 28–42.

Yanai, T., Hay, J.G., Gerot, J.T., 1996. Three-dimensional videography with panning periscopes. Journal of Biomechanics 29, 673–678.